J Mater Sci (2009) 44:5795–5799
DOI 10.1007/s10853-009-3813-0

On the determination of elastic modulus in very stiff materials by depth sensing indentation

A. Rico · M. A. Garrido Maneiro · M. T. Gómez Del Rio · A. Salazar · J. Rodríguez

Received: 27 April 2009 / Accepted: 14 August 2009 / Published online: 29 August 2009

Abstract Depth sensing indentation tests were carried out in stiff ceramics like Al_2O_3, AlN, SiC and B_4C, using a diamond Berkovich tip. The experiments show that the accuracy of the data depends on the stiffness ratio between material and indenter. An iterative calibration procedure is proposed to get a reliable estimation of the elastic modulus.

Introduction

Depth sensing indentation is the most appropriate, and sometimes the only available, technique to determine surface mechanical properties. A method proposed by Oliver and Pharr is extensively used to analyse the experimental data and to obtain elastic modulus, E, and hardness, H, of the sample [1]. These properties are calculated from the load–displacement curves, P–h, according to the following expressions:

$$H = \frac{P_{\max}}{A} \tag{1}$$

where $P_{\max}$ is the maximum load and A is the projected area of contact at maximum load. On the other hand,

$$E^* = S\frac{1}{2}\frac{\sqrt{\pi}}{\sqrt{A}}\frac{1}{\beta} \tag{2}$$

where S is the unloading stiffness evaluated at maximum displacement, $h_{\max}$.

A. Rico · M. A. Garrido Maneiro · M. T. Gómez Del Rio · A. Salazar · J. Rodríguez (✉)
Departamento de Ciencia e Ingeniería de Materiales, Universidad Rey Juan Carlos, C/Tulipán s/n 28933 Móstoles, Madrid, Spain
e-mail: jesus.rodriguez.perez@urjc.es

$$S = \left[\frac{dP}{dh}\right]_{(h=h_{\max})} \tag{3}$$

β is a constant dependent on the indenter geometry and E^* is the reduced or effective modulus determined by:

$$\frac{1}{E^*} = \frac{1-\nu^2}{E} + \frac{1-\nu_i^2}{E_i} \tag{4}$$

where E, ν, E_i and ν_i represent Young's modulus and Poisson ratio of the material and the indenter, respectively. In the preceding expressions, the projected contact area, A, is evaluated through the indenter shape function, $A = A(h_p)$, a relationship between A and the contact depth, h_p ($A = 24.5\ h_p^2$, for an ideal Berkovich tip). Finally, this magnitude can be calculated from the expression:

$$h_p = h_{\max} - \varepsilon\frac{P_{\max}}{S} \tag{5}$$

where ε is again a constant dependent on the indenter geometry.

Many practitioners of nanoindentation simply use the Oliver and Pharr method without paying attention to its limitations. Actually, this procedure is problematic in handling soft materials, due to viscoelastic effects [2–4], and also very stiff materials as it will be pointed out in this work. Curiously, the Oliver and Pharr method is reasonably applicable to a range of materials, which are mostly metals, which are neither too soft nor too stiff. Examples of successful characterisation of metallic materials [5, 6] or ceramics by depth sensing indentation can be found elsewhere [7].

To get consistent results in applying this procedure, an accurate knowledge of the contact geometry is essential. Deviations from the theoretical contact geometry not taken into account could produce miscalculations in H and E. Tip deformation or roundness are artefacts with nothing to do

with the material tested, but leading to inaccurate values if no corrections are applied [8].

One of the problems still unsolved is the deviation from the theoretical conditions due to the indenter deformation and the consequent alteration of the contact geometry. When the stiffness of the indented material is comparable to that of the indenter, the actual conditions are far away from the assumptions considered in the data analysis. Several authors carried out finite element simulations of indentation tests, and concluded that the deformation of the tip could lead to a large error in the values of the mechanical properties when a very stiff material is indented, due to a bad estimation of the contact area [9, 10]. This effect becomes more relevant when the material stiffness tends towards that of the indenter, like in the stiff ceramics tested in this work. This research is focused on this subject, especially on the determination of elastic modulus when ceramic materials are indented at nanometric scale.

Materials and experimental techniques

Alumina, aluminium nitride, silicon carbide and boron carbide from which the mechanical properties are known, were indented using a diamond Berkovich tip with a nominal edge radius of 20 nm. Table 1 shows the nominal properties of these materials together with those of the diamond [11]. The experimental device used was a Nanoindenter XP (MTS System Co.). The instrument applies load via a calibrated electromagnetic coil with a resolution of 50 nN. The displacement of the indenter is measured using a capacitive transducer with a resolution of 0.01 nm. Twenty series of indentation tests and ten tests per each one were carried out at different maximum loads from 1 to 500 mN for all materials. Before the tests, a calibration of the tip was made in silica following the traditional methodology, i.e. a series of indentations were done at different contact depths in a material where the modulus is known. Using Eq. 2, the function which provides the contact area, A, versus the contact depth, h_p, is obtained [12]. This function for Berkovich tips usually takes the form:

$$A = 24.5h_p^2 + C_1h_p + C_2h_p^{1/2} + C_3h_p^{1/4} + C_4h_p^{1/8} + \ldots \quad (6)$$

where C_i are fit constants.

Results and discussion

According to the calibration in silica using Eq. 6 and following the Oliver and Pharr procedure, the results in Fig. 1a were obtained. A strong dependence of the elastic modulus with the indentation size is observed in all the materials tested. In some cases like SiC or B_4C the values obtained are clearly overestimated in comparison with the reference values [11]. This behaviour cannot be justified by physical arguments and the possibility of inconsistencies of the method should be considered.

Although the Eq. 6 takes into account the non-ideal geometry of the indenter, the method is based on the assumption of mechanical equivalence between real Berkovich and ideal conical tips. The data at low penetration depths are affected by the tip roundness. The relationship between the elastic displacement, h_e, and the load, P, during unloading depends on the tip geometry and is given by the following law:

$$P = Kh_e^m \quad (7)$$

Spherical tips obey a power law with an exponent equal to 1.5 [13]. However, if the geometry corresponds to a cone the exponent is 2, according to Sneddon work [14].

Figure 1b shows an example of the data fit at low loads and Fig. 1c the corresponding fit to high loads. The best fit of the exponent m in Eq. 7 is shown in Fig. 1d versus penetration depth for the materials studied. A transition

Table 1 Properties and results obtained in the studied materials

Material	Al_2O_3	AlN	SiC	B_4C	Diamond
Young's modulus (GPa)	325	340	420	460	1140
Poisson coefficient	0.28	0.25	0.18	0.20	0.07
Vickers hardness (GPa)	18	12	23	34	85
Compression yield strength (GPa)	2.6	–	2.5	–	–
Relative density (%)	96.0	98.0	99.0	99.7	–
Grain size (μm)	2.4	–	3.3	–	–
Radius of the plastic zone (μm)[a]	4.22	–	6.7	–	–
Number of grains inside the plastic zone[a]	22	–	33	–	–
B_j from fitting $A = B_j h_p^2$ (R^2 coefficient)	22.66 (0.9992)	23.86 (0.9998)	–	30.63 (0.9976)	–

[a] To make these calculus the lowest total penetration associated with an exponent $m = 2$ is used in each material

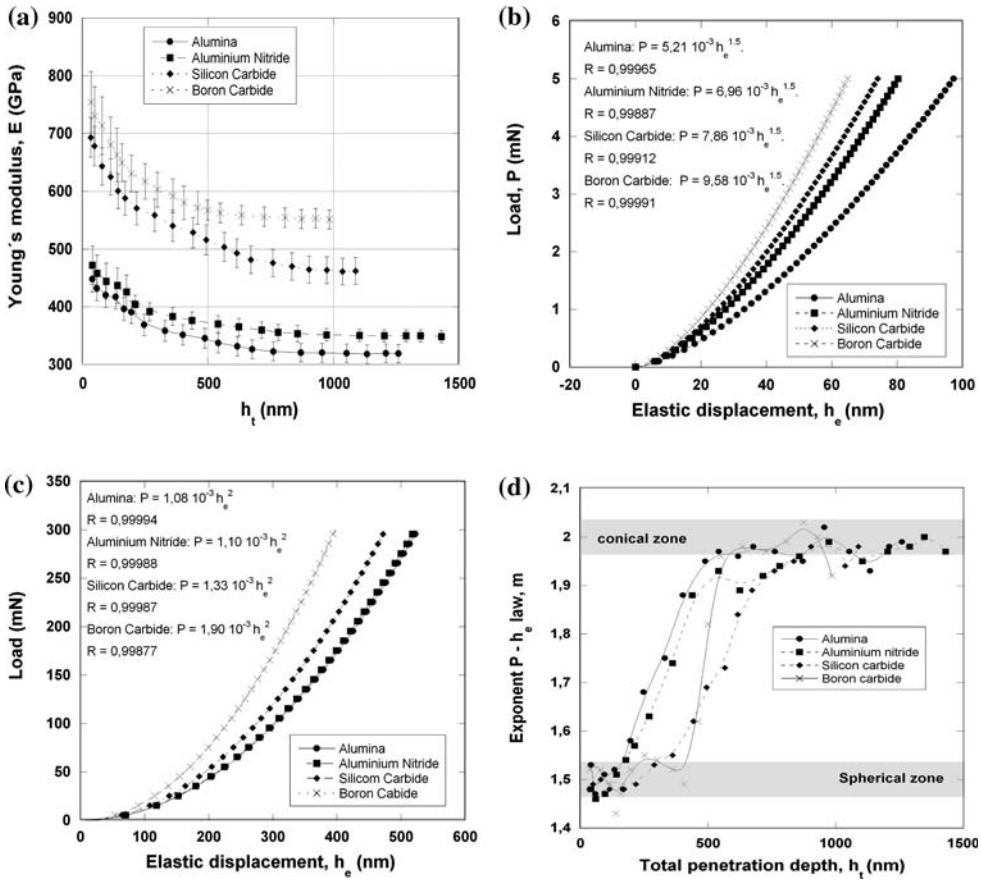

Fig. 1 **a** Elastic modulus versus total depth of penetration, **b** examples of P–h_e data fit at lower penetrations, **c** examples of P–h_e data fit at higher penetrations, **d** exponent of the best fit in the P–h_e law versus total penetration depth

between regions dominated by spherical and conical contact is observed in all cases, but the transition is retarded for stiffer materials. At low loads, the equations controlling the indentation correspond mainly to spherical contact and, then, the solution developed in the Oliver and Pharr method for Berkovich tips should not be used to obtain consistent mechanical properties.

This transition between low and high penetration depths suggests the possibility of an alternative explanation quite far from the tip geometry. The differences observed may be due to the hypothesis of isotropy that supports the analysis done. If the indentation affects just one or a few grains an anisotropic approach should be used [15]. Only in the case of many grains were affected by the indentation, the Eqs. 1–7 are valid. The question of what grains are or not affected by the indentation is not easy to answer in a real material. Chen and Bull [16] have recently performed a finite element modelling of a conical indentation and derived a relationship between the plastic zone radius, R_p, and the indentation depth, h_t, according to the following expression:

$$\frac{R_p}{h_t} = \sqrt{\frac{0.3\pi E_r}{Y}}\left(\sqrt{\frac{1}{\pi \tan^2\theta}}\sqrt{\frac{E_r}{H}} + \varepsilon\sqrt{\frac{\pi}{4}}\sqrt{\frac{H}{E_r}}\right)^{-1} \quad (8)$$

where Y is the material yield strength, θ, the effective half included angle, i.e. 70.3° for a Berkovich tip, and the rest of magnitudes have been previously defined in Eqs. 1–7. The application of Eq. 8 to our materials and the estimated number of grains inside the plastic zone are included in Table 1 for alumina and SiC (the only two materials for which all the relevant data were available). The results obtained support that, in the so-called conical region, the isotropy hypothesis is consistent.

Consequently, due to either the tip geometry or to the anisotropy of the indentations at low depths, the analysis following the Oliver and Pharr procedure should be limited to those data controlled by an exponent 2 in Eq. 7. But even if this precaution is taken, the elastic modulus predicted is not coincident with the nominal one. The effect of the tip deformation is not yet corrected.

If the stiffness of the reference material used in the tip calibration is not similar to that of the material indented, the relationship between contact area and contact depth would be different and the calibration function useless. So, in a first approximation a calibration in materials with similar stiffness than the target material could be a possible solution. Figure 2 shows the results obtained from the experiments in silicon carbide after a calibration (Eq. 6)

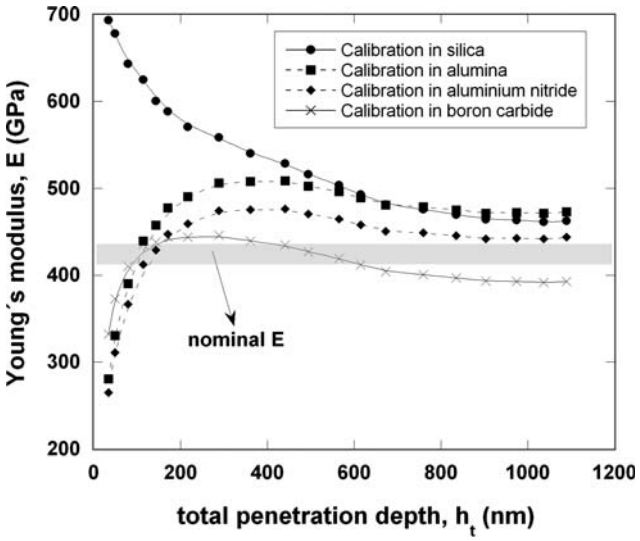

Fig. 2 Elastic modulus versus total penetration depth of silicon carbide calculated using calibration in silica, alumina, aluminium nitride and boron carbide

using the other ceramics tested as reference materials. The findings are rather unsatisfactory. The values obtained exhibit size dependence, although the variation with the total displacement, h_t, is different depending on the reference material used to calibrate the tip. When the reference material is stiffer than the material indented, the contact area is overestimated because of the strain induced on the indenter during calibration. The consequence is the underestimation of the elastic modulus. If the reference material is more compliant than the sample, the opposite trend is observed.

The estimation of the contact area is highly dependent on the material stiffness. Strictly speaking, the true contact area could only be precisely determined if the calibration is done in reference materials with mechanical properties very similar to those of the object of analysis. Certainly, that would mean to know in advance the properties to be determined by depth sensing indentation. As this is mostly impracticable, another methodology is required to get reliable properties.

To consider the tip deformation, a different calibration strategy should be followed. Equation 6 employs 24.5 as a fix coefficient of the h_p^2 plus additional terms, according to the theoretical description of a contact dominated by a conical geometry. In the alternative procedure here proposed, Eq. 6 has been substituted by:

$$A = Bh_p^2 \quad \text{with } B = f\left(E/E_i\right) \tag{9}$$

The Eq. 9 seems to be simpler than 6, but actually the constants C_i have been replaced by a function $f(E/E_i)$, dependent on the ratio between the elastic modulus of material, E, and indenter, E_i and calculated from fitting the experimental data. The function f contains information regarding the tip deformation. The results of this approach are included in Table 1, where only data coming from the region controlled by an exponent $m = 2$ were used. Data from SiC have been excluded because this material was reserved to perform a final check of the method.

In a first approximation, a linear variation can be considered. Data from Al_2O_3, AlN and B_4C exhibit good agreement ($R^2 = 0.9958$) with the expression:

$$B = f\left(E/E_i\right) = 3.79 + 66.35\left(E/E_i\right) \tag{10}$$

Evidently, this is not a universal relationship, but only representative of the tip used in the range where the calibration was performed. Subsequent refinements of this calibration function can be obtained if more reference materials are added. The relevant point is not the function itself, but the need to change the calibration according to the relative stiffness of the material tested. The application of Eq. 9 to the materials used as reference in the new calibration (Al_2O_3, AlN and B_4C) is shown in Fig. 3.

The function f is used as a step of an iteration method described in the scheme showed in Fig. 4. An initial value of the elastic modulus is taken from the original experimental data, E_j (from the conical region of Fig. 1a). The calibration function f is fed by the E_j/E_i ratio and B_j coefficient is then calculated using Eq. 10. The new contact area is then computed using B_j coefficient in Eq. 9. Following the Oliver and Pharr method is possible to find a new E_{j+1}. Then, the E_{j+1}/E_i value is used as the initial value for the next iteration. Elastic moduli are plotted versus the number of iteration in Fig. 5. The reliability of the procedure proposed is proved with AlN data and, especially, with SiC results, not used as reference material

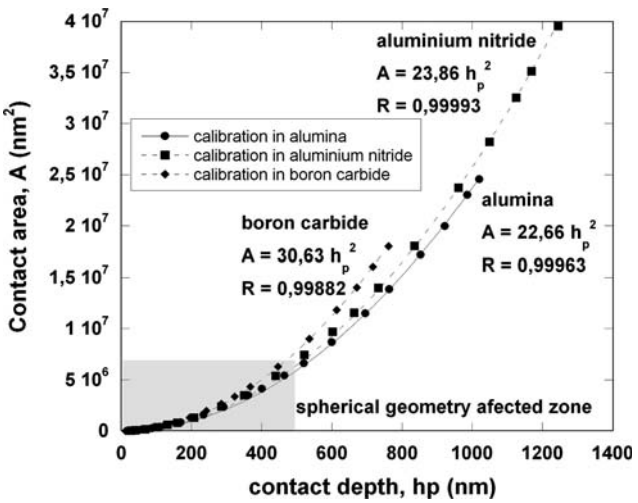

Fig. 3 Application of Eq. 9 to the materials used in the new calibration procedure. Data coming from the spherical region are excluded of the data fit

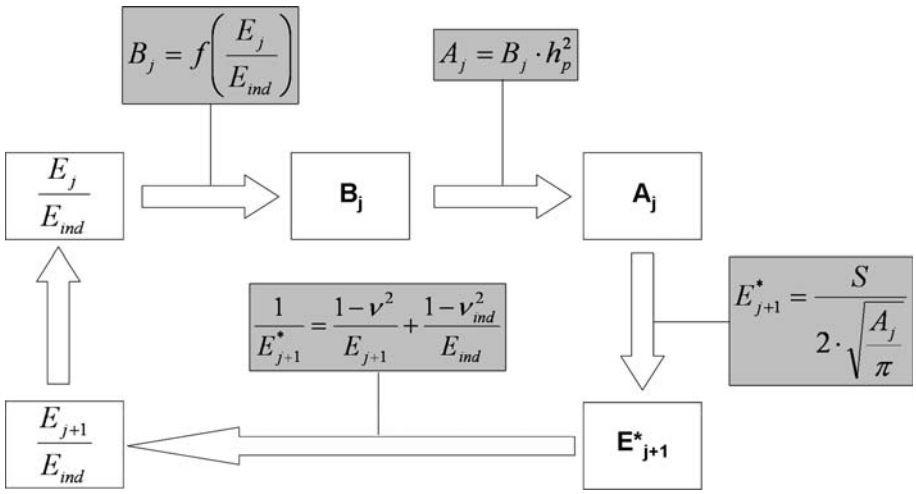

Fig. 4 Scheme of the iteration process proposed

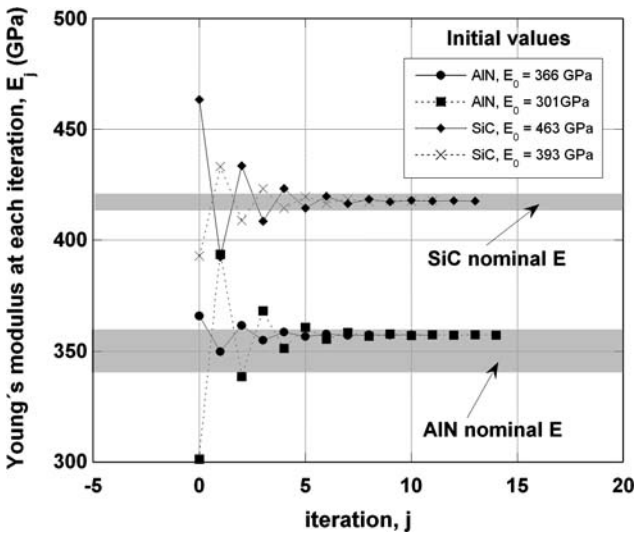

Fig. 5 Evolution of the elastic modulus during the iteration process considering several initial values

during the calibration. As it can be observed, the iterative procedure converges to the nominal elastic modulus independently on the starting value. Only data coming from the region dominated by the conical contact were analysed following this method. Data from spherical region need to be studied in a different way and more research is needed to reach a suitable procedure.

Summary

The elastic moduli of very stiff materials measured by depth sensing indentation with Berkovich indenters are affected by tip roundness and tip deformation. Tip roundness effect can be avoided analysing the unloading branch of the load–displacement curve. The exponent of the power relationship between load and elastic displacement allows discriminating the regions dominated by spherical or conical contact. Deformation of the indenter can be overcome through an iteration method based on a calibration function drawn from fitting the parameter B expressed in Eq. 9, which includes the information related to the deformation of the indenter due to the stiffness ratio between the material and the indenter. This alternative method should be used when testing stiff materials and when a significant size dependency in the elastic modulus values is observed.

Acknowledgement The authors are indebted to Comunidad de Madrid for the financial support through program ESTRUMAT.

References

1. Oliver WC, Pharr GM (1992) J Mater Res 7:1564
2. Feng G, Ngan AHW (2002) J Mater Res 17(3):660
3. Ngan AHW, Tang B (2002) J Mater Res 17(10):2604
4. Tang B, Ngan AHW (2003) J Mater Res 18(5):1141
5. Mussert KM, Vellinga WP, Bakker A, Van der Zwaag S (2002) J Mater Sci 37:789. doi:10.1023/A:1013896032331
6. Gómez del Río T, Poza P, Rodríguez J (2005) J Mater Sci 40:1513. doi:10.1007/s10853-005-0594-y
7. Twigg PC, Riley FL (2002) J Mater Sci 37:845. doi:10.1023/A:1013812503198
8. Yu N, Polycarpou AA, Conry TF (2004) Thin Solid Films 450:295
9. Knapp JA, Follstaedt DM, Myers SM, Barbour JC, Friedmann TA (1999) J Appl Phys 85:1460
10. Faulkner A, Tang KC, Sen S, Arnell RD (1998) J Strain Anal 33:411
11. Galvez F (1999) Mechanical characterization of advanced ceramic materials at high strain rates. Doctoral Thesis, Polytechnic University of Madrid
12. McElhaney KW, Vlassak JJ, Nix WD (1997) J Mater Res 13(5):1300
13. Hertz H (1882) On the contact of rigid elastic solids and on hardness. Verhandlungen des Vereins zur Beförderung des Gewerbefleisses, Leipzig, Berlin, p 90
14. Sneddon IN (1965) Int J Eng Sci 3:47
15. Vlassak JJ, Nix WD (1994) J Mech Phys Solids 42(8):1223
16. Chen J, Bull SJ (2006) Surf Coat Technol 201:4289